Published in final edited form as:
Neuron. 2007 June 21; 54(6): 949–959. doi:10.1016/j.neuron.2007.06.002.

Differential expression of post-tetanic potentiation and retrograde signaling mediate target-dependent short-term synaptic plasticity

Michael Beierlein, **Diasynou Fioravante**, and **Wade G. Regehr***
Department of Neurobiology, Harvard Medical School, Boston, MA 02115

Summary

Short-term synaptic plasticity influences how presynaptic spike patterns control the firing of postsynaptic targets. Here we investigated whether specific mechanisms of short-term plasticity are regulated in a target-dependent manner, by comparing synapses made by cerebellar granule cell parallel fibers onto Golgi cells (PF→GC synapse) and Purkinje cells (PF→PC synapse). Both synapses exhibited similar facilitation, suggesting that any differential short-term plasticity does not reflect differences in the initial release probability. PF→PC synapses were highly sensitive to stimulus bursts, which could result in either depression of subsequent responses, mediated by endocannabinoid-dependent retrograde signaling, or enhancement of responses through post-tetanic potentiation (PTP). In contrast, stimulus bursts had remarkably little effect on the strength of PF→GC synapses. Unlike PCs, GCs were unable to regulate their PF synapses by releasing endocannabinoids. Moreover, PTP was reduced at the PF→GC synapse compared to the PF→PC synapse. Thus, the target-dependence of PF synapses arises from the differential expression of both retrograde signaling and PTP.

Keywords

Munc13; PKC; DSE; DSI; augmentation; paired-pulse facilitation; mGluR

Introduction

Short-term synaptic plasticity modulates how presynaptic patterns of action potentials control the firing of postsynaptic targets (Abbott and Regehr, 2004; Destexhe and Marder, 2004; Markram et al., 1998a). Synapses exhibit diverse forms of short-term plasticity that reflect the interplay of numerous mechanisms (Magleby, 1979; Zucker, 1996; Zucker and Regehr, 2002). Consequently, synapses can perform computations by filtering spike trains in distinctive ways (Silberberg et al., 2005; von Gersdorff and Borst, 2002). As a given neuron usually synapses onto numerous types of neurons, a particularly interesting issue is the extent to which synaptic properties are specifically tailored to allow the same presynaptic pattern of activity to influence the firing of different types of targets in distinctive ways.

*To whom correspondence should be addressed: Wade Regehr, Goldenson 308, Department of Neurobiology, Harvard Medical School, 220 Longwood Avenue, Boston, MA 02115, Tel: 617-432-0435, Fax: 617-734-7557, wade_regehr@hms.harvard.edu.

Previous studies have established that both short- and long-term forms of synaptic plasticity can be controlled by the postsynaptic target (Markram et al., 1998b; Pelkey et al., 2005; Pouille and Scanziani, 2004; Reyes et al., 1998; Rozov et al., 2001; Thomson, 1997; Toth et al., 2000). For example, the properties of long-term plasticity at hippocampal mossy fiber synapses made by granule cells differ on CA3 pyramidal cells and on interneurons (Pelkey et al., 2005). In the hippocampus and neocortex, the initial probability of release (*p*) of individual inputs is often target-specific (Losonczy et al., 2002; Markram et al., 1998b; Reyes et al., 1998; Scanziani et al., 1998; Thomson, 1997). This can lead to differences in short-term plasticity, because synapses with high *p* and low *p* are associated, respectively, with short-term depression and facilitation (Thomson, 2000). Moreover, the differential presynaptic activation of ionotropic or metabotropic receptors (Delaney and Jahr, 2002; Gao and Goldman-Rakic, 2003; Khakh et al., 2003; Scanziani et al., 1998; Shigemoto et al., 1997) can allow for the dynamic regulation of synaptic strength. However, the extent to which specific mechanisms of short-term plasticity can be regulated directly and independently of initial *p* in a target-dependent manner is unclear.

Distinct mechanisms can govern target-specific short-term synaptic plasticity (Magleby, 1979; Zucker and Regehr, 2002). Activation of synapses with pairs of stimuli leads to depression or facilitation of neurotransmitter release that lasts for hundreds of milliseconds. Bursts of presynaptic activity trigger a build-up of calcium in presynaptic boutons (Delaney and Tank, 1994; Delaney et al., 1989; Zucker, 1996) resulting in longer-lasting forms of plasticity, such as augmentation and post-tetanic potentiation (PTP). Moreover, brief bursts can promote the release of endocannabinoids (eCBs) from postsynaptic cells, activating presynaptic CB1 receptors to suppress neurotransmitter release (Brown et al., 2003; Chevaleyre et al., 2006).

Here we tested whether any of these mechanisms of short-term plasticity are regulated by the postsynaptic target. We compared synapses made by the parallel fibers of cerebellar granule cells onto Purkinje cells (PF→PC synapse) and Golgi cells (PF→GC synapse). We found that both synapses exhibit similar facilitation, which suggests that the initial *p* at these synapses is similar. Previous studies have demonstrated that at PF→PC synapses stimulus bursts can lead to either potentiation of transmitter release, or they can cause PCs to release eCBs, which leads to retrograde suppression (Brenowitz and Regehr, 2005; Brown et al., 2003; Marcaggi and Attwell, 2005). Here we show that stimulus bursts have remarkably little effect on synaptic strength at PF→GC synapses. In part this is because GCs are unable to regulate synaptic strength by releasing endocannabinoids. Moreover, the magnitude of PTP is much smaller at the PF→GC synapse than at the PF→PC synapse. Therefore, target-dependent differences of granule cell PF synapses arise from a combination of presynaptic and postsynaptic specializations that regulate specific mechanisms of short-term plasticity.

Results

Target-dependent changes in synaptic strength

We examined changes in synaptic strength following brief stimulus bursts at parallel fiber (PF) synapses formed onto two postsynaptic targets (Figure 1A), Purkinje cells (PCs, Figure 1B) and Golgi cells (GCs, Figure 1H). Previous in vivo studies have shown that granule cells can fire in high-frequency bursts (Chadderton et al., 2004; Jorntell and Ekerot, 2006). In turn, brief PF bursts can activate postsynaptic type 1 metabotropic glutamate receptors (mGluR1s) in PCs (Batchelor and Garthwaite, 1997; Tempia et al., 1996), due to glutamate pooling and spill-out from the synaptic cleft. Activation of mGluR1 triggers the release of eCBs (Brown et al., 2003; Maejima et al., 2001), ultimately resulting in synaptically-evoked suppression of excitation (SSE). SSE is shown in a representative experiment in Figure 1C–1E. A stimulus electrode was placed in the molecular layer (ML) and PF EPSCs were

evoked at low frequencies in voltage clamp (Figure 1D, *left*). PFs were then stimulated with a brief train (10 stimuli, 50 Hz) and the PC response was measured in current clamp (Figure 1C) to allow the cell to depolarize and generate action potentials. The recording was then returned to voltage clamp and low frequency PF activation resumed. PF bursts evoked by ML stimulation led to a strong and transient suppression of EPSCs (Figure 1D and 1E, *black traces*). We then placed the stimulus electrode in the granular layer (GrL) to activate PF inputs that are more spatially dispersed, thereby minimizing glutamate pooling and spill-out from the synaptic cleft, which for similar EPSC amplitudes should result in a smaller degree of mGluR1 activation as shown previously (Marcaggi and Attwell, 2005). Under these conditions, PF bursts led to a strong and transient synaptic enhancement (Figures 1E, 1G, *red traces*), while the response evoked by the PF bursts remained similar (Figure 1F). Thus, for PCs, synaptic strength following PF bursts shows pronounced suppression or enhancement, depending on the degree of postsynaptic mGluR activation (Marcaggi and Attwell, 2005). Similar properties have been observed for PF synapses onto molecular layer interneurons (Beierlein and Regehr, 2006).

We then investigated burst-evoked changes in synaptic strength at the PF to GC synapse (Figures 1I–1M). When PFs were activated in the ML, bursts of PF inputs did not lead to suppression of excitation (Figures 1J and 1K, *black traces*), contrary to what we observed for PCs. Moreover, when spatially dispersed PF inputs were activated with GrL stimulation, very little change in synaptic strength was observed (Figures 1K and 1M, *red traces*). Thus, PF inputs to GCs display a narrower dynamic range compared to inputs to PCs. In the following, we will examine in detail the mechanisms underlying this target-dependent plasticity.

PF to GC synapses express CB1Rs, but do not display eCB-mediated SSE or DSE

The above data indicate that PF→GC synapses do not display SSE, suggesting that GCs may not release eCBs in response to synaptic activity. To test for a role of eCBs in synaptic plasticity at the PF→GC synapse, we compared changes in synaptic strength following PF bursts in the ML (cf. Figures 1K–1M), in the absence and presence of the CB1 receptor (CB1R) antagonist AM251. Under control conditions, synaptic strength following PF bursts was slightly enhanced (Figures 2A and 2B). The extent of enhancement was unaffected by AM251, suggesting that under our experimental conditions synaptic activity does not lead to eCB-mediated changes in synaptic strength. This lack of involvement of eCBs in plasticity at the PF→GC synapse contrasts with the PF→PC synapse, which is highly sensitive to eCB release (Figure 2C, Brown et al., 2003).

We performed additional experiments to determine why eCB-mediated plasticity is absent at PF→GC synapses. The majority of GCs do not express postsynaptic mGluR1s (Knoflach et al., 2001; Watanabe and Nakanishi, 2003), which play a crucial role in SSE at the PF→PC and other synapses (Chevaleyre et al., 2006). We therefore examined depolarization-induced suppression of excitation (DSE), as DSE is driven solely by high calcium levels (Brenowitz and Regehr, 2003) and does not rely on activation of metabotropic receptors (Brenowitz et al., 2006). We tested for DSE in GCs by recording from neurons with a Cs-based internal solution and monitoring PF EPSC amplitudes prior to and following a 2 s depolarizing step to 0 mV (Figure 2D). In contrast to PCs (Figure 2F), no DSE was observed in GCs (Figure 2E). Furthermore, bath application of AM251 had no effect on EPSC amplitudes following voltage steps (Figure 2E). Depolarizing steps of longer duration also failed to evoke DSE. EPSC amplitudes following 5 s depolarizing steps to 0 mV were 0.95 ± 0.02 of control (n = 11). We also measured dendritic calcium transients in GCs and found that in all cells tested, postsynaptic depolarizations of 2 s duration led to calcium increases of ~ 10 μM (Figures 3A and 3B), which are larger than the calcium concentrations of ~7 μM and ~4 μM required for half-maximal DSE at PF→PC synapses (Brenowitz et al., 2006) and half-maximal DSI in

hippocampal pyramidal cells (Wang and Zucker, 2001), respectively. Thus, the lack of DSE at the PF to GC synapse is unlikely to be caused by insufficient dendritic calcium elevations. These findings suggest that the lack of retrograde inhibition at PF→GC synapses cannot be explained solely by the lack of mGluR1s in GCs.

The absence of SSE and DSE at the PF→GC synapse could arise from either the inability of GCs to synthesize and release eCBs, or from the absence of presynaptic CB1Rs. To distinguish between these possibilities, we recorded PF-evoked EPSCs in GCs and bath-applied the CB1R agonist WIN 55,212-2 (Figure 3C). WIN led to a reduction in EPSC amplitude in all cells (Figure 3D), which was reversed by applying AM251 (n = 5). To determine whether this effect was mediated by presynaptic CB1Rs, PF synapses were stimulated with pairs of stimuli under control conditions and following application of WIN. WIN led to increased paired-pulse facilitation at PF→GC synapses (Figures 3E and 3F), whereas postsynaptic depolarization, which reliably increases paired-pulse facilitation at the PF→PC synapse (Kreitzer and Regehr, 2001), remained ineffective (Figure 3F). These data show that PF terminals onto GCs indeed express CB1Rs.

Studies in hippocampal pyramidal cells indicate that DSI can be more prominent than DSE, due to a higher expression of CB1Rs at inhibitory synapses (Ohno-Shosaku et al., 2002). It is not known whether excitatory and inhibitory terminals in the cerebellum show differential sensitivity to eCBs. To test whether eCBs released from GCs influence inhibitory terminals selectively we attempted to evoke DSI in GCs. However, following depolarizing steps of 2s duration, the amplitude of evoked IPSCs remained virtually unchanged when compared to control (0.97±0.04, n=5).

In summary, these data show that presynaptic CB1Rs are present at PF→GC synapses. The absence of SSE, DSE and DSI suggests that GCs do not release sufficient eCBs to suppress transmission. Moreover, the lack of SSE indicates that eCBs released from neighboring PCs do not activate CB1Rs on PF terminals onto GCs.

Target-dependent differences in synaptic enhancement and PTP

Our data above (Figures 1, 2B and 2C) indicate that PF synapses onto GCs differ from those onto PCs not only in their lack of SSE but also in their lack of post-tetanic enhancement. This suggests that, in addition to postsynaptic differences at the two PF synapses, there are target-dependent specializations in presynaptic mechanisms. Forms of post-tetanic enhancement lasting 10 seconds to minutes have been observed at many synapses, and are known as either augmentation or post-tetanic potentiation (PTP, Magleby, 1979; Zucker, 1996; Zucker and Regehr, 2002). The distinction between these different forms of plasticity is not always clear, particularly when making comparisons across different synapses. Here we refer to the post-tetanic enhancement following stimulus bursts at PF synapses as PTP.

We characterized presynaptic forms of short-term plasticity by recording from cells in voltage clamp, in the presence of $GABA_A$, $GABA_B$, and CB1 receptor antagonists to block the effects of GABA and eCB signaling. We first measured paired-pulse plasticity at PF synapses onto PCs and GCs, to determine whether they show targetdependent differences in initial release probability (*p*). Both synapses displayed pairedpulse facilitation with a similar amplitude and time course (Figures 4A and 4B) suggesting that *p* is similar for PF synapses onto PC and GCs.

We then studied PTP evoked by stimulus trains (10 stimuli, 50 Hz). Differences in short-term plasticity were apparent during (Figures 4C and 4D) and following (Figures 4E and 4F) stimulus trains. For PF→PC synapses, synaptic enhancement built up over the course of the stimulus train, with a maximal enhancement at the end of the train (Figure 4C, *black trace*).

In contrast, enhancement in PF→GC synapses peaked for the third response, and had a smaller steady-state amplitude at the end of the train (Fig. 4C, *red trace*, $EPSC_{10}/EPSC_1$ = 3.7 ± 0.3, n = 14 for PCs; 1.7 ± 0.2, n = 13 for GCs). Furthermore, the magnitude of PTP differed dramatically for the two synapses (Figures 4E and 4F). On average, EPSCs in PCs 1 s after the onset of the stimulus burst were enhanced by 92 ± 8% (n = 10) and returned to baseline with a time course that was approximated with an exponential decay with τ = 11.3 s (Figure 4E). The enhancement of GC EPSCs was only 26 ± 4% (n = 17) and it decayed with a time constant of 11.3 s.

If PTP is mediated by an increase in release probability, paired-pulse facilitation should be reduced following a stimulus burst, with a time course similar to the increase in synaptic strength (McNaughton, 1982; Zucker and Regehr, 2002). Indeed, paired-pulse facilitation was reduced in PCs following bursts and recovered with a time course similar to the recovery in EPSC amplitude (Figures 5A and 5B). This suggests that PTP at PF synapses reflects an increase in *p*. By contrast, the paired-pulse ratio at the PF→GC synapse was virtually unchanged following stimulus bursts (Figures 5B and 5C), indicating that the smaller magnitude of PTP at this synapse was a consequence of a smaller increase in transmitter release compared to PF→PC synapses.

Several findings suggest that differences in PTP at synapses onto GCs and PCs were neither secondary to differences in the initial *p*, nor a consequence of postsynaptic factors. First, a plot of the magnitude of PTP vs. the initial paired-pulse ratio for each experiment performed under control conditions showed clear differences in the magnitude of PTP at the two synapses regardless of the extent of paired-pulse facilitation (Figure 6A). Second, when *p* was lowered by reducing the external calcium concentration to 1 mM, facilitation was more pronounced at the PF→GC synapse, but PTP was unchanged (Figure 6B, *red squares*). At the PF→PC synapse an increase in PTP was also observed (Figure 6B, *black squares*), and thus the difference in the magnitude of PTP for synapses onto GCs and PCs became more pronounced. Third, experiments in the presence of the low affinity AMPAR antagonist DGG indicated that AMPAR saturation does not account for differences in PTP at the two synapses (Figure 6B, *triangles*). Because DGG has rapid kinetics, it has been widely used to relieve AMPAR saturation (Foster et al., 2005; Wadiche and Jahr, 2001). We found that in the presence of DGG, paired-pulse facilitation was enhanced for both synapses, indicating the presence of AMPAR saturation. However, differences in PTP persisted even in the absence of AMPAR saturation. In summary, these data show that PTP can differ dramatically in a target-dependent manner, even when initial *p* is similar.

The mechanism of PTP at PF synapses

Studies from a number of systems indicate that PTP is driven by elevations in presynaptic calcium, in a range of hundreds of nanomolar (Delaney et al., 1989; Zucker, 1996). This residual calcium signal is thought to interact with a high-affinity binding site that ultimately leads to increased release probability. Two candidate presynaptic mechanisms have been implicated in PTP and related forms of short-term enhancement: Munc13, a family of vesicle priming factors (Augustin et al., 1999b; Betz et al., 1998; Brose et al., 1995; Brose and Rosenmund, 2002; Rosenmund et al., 2002), a signaling cascade involving protein kinase C (PKC, Alle et al., 2001; Brager et al., 2003) or both pathways (Wierda et al., 2007). We used knockout mice and pharmacology to examine a potential role of these proteins in PTP at PF synapses.

Three Munc13 isoforms are expressed in the brain (Augustin et al., 1999a), and differential expression of these isoforms is thought to regulate short-term plasticity (Rosenmund et al., 2002). Both Munc13-1 and Munc13-3 are strongly expressed in cerebellar granule cells, while Munc13-2 is only weakly expressed in the cerebellum (Augustin et al., 1999a).

Although mice lacking Munc13-1 do not survive, mice lacking Munc13-3 are viable. This difference in viability likely reflects the fact that Munc13-1 is strongly expressed throughout the brain whereas Munc13-3 has a more restricted pattern of expression (Augustin et al., 2001). Munc13-3 knockout mice show small increases in paired-pulse plasticity at the PF to PC synapse (Augustin et al., 2001), but it is not known if Munc13-3 deletion affects PTP and it is unclear whether the role of Munc13-3 is limited to PF to PC synapses.

We therefore compared paired-pulse plasticity, short-term enhancement during trains and the magnitude of PTP for PF synapses onto PCs and GCs, in Munc13-3 knockout mice and their wild-type littermates (Figure 7). In contrast to rats, PF synapses in wild-type mice displayed target-dependent differences in paired-pulse facilitation, with initial *p* being higher at PF→GC synapses than at PF→PC synapses (Figure 7B, cf. 4A). However, similar to rats, in wild-type mice PTP remained more prominent for synapses onto PCs than for synapses onto GCs (Figures 7E and 7F, *black symbols*). Compared to wild-type mice, PF→PC synapses in Munc13-3 knockout animals displayed slightly enhanced paired-pulse plasticity (Figure 7A) but little change in short-term enhancement during stimulus trains (Figure 7C), in agreement with previous results (Augustin et al., 2001). In contrast, for PF→GC synapses Munc13-3 deletion led to a more pronounced increase in paired-pulse plasticity (Figure 7B) and a large enhancement during stimulus trains (Figure 7D). The observed increase in the extent of facilitation at both synapses is consistent with the proposed role of Munc13-3 in synaptic vesicle priming (Augustin et al., 2001).

Although the deletion of Munc13-3 influenced paired-pulse facilitation and thus initial *p*, it had no effect on the properties of PTP (Figures 7E and 7F). Compared to wild-type mice, the magnitude and time course of PTP in Munc13-3 knockout animals remained unchanged at both synapses. Thus, Munc13-3 at PF synapses appears to regulate initial *p*, but has no apparent role in determining the properties of PTP.

We then tested whether PKC is required for PTP at PF synapses in rats. Slices were incubated in the specific PKC inhibitor GF 109203X (Toullec et al., 1991) for 1 hr and responses were recorded in the continued presence of the drug. Paired-pulse facilitation (Figures 8A and 8B) and short-term enhancement in response to stimulus trains (Figures 8C and 8D) were unchanged relative to control conditions for both types of PF synapses, suggesting that initial *p* and presynaptic calcium dynamics were not affected by the drug. However, for PF synapses onto both PCs and GCs, PTP was eliminated (Figures 8E and 8F). The decrease in paired-pulse facilitation that accompanied PTP in control conditions ($EPSC_2$ / $EPSC_1$ = 2.3 ± 0.1 pre-burst; 1.5 ± 0.1 at 1 s post-burst, n = 9) was greatly attenuated when PTP was eliminated by GF 109203X ($EPSC_2$ / $EPSC_1$ = 2.3 ± 0.1 pre-burst; 2.0 ± 0.1 at 1 s post-burst, n = 7), independently confirming the presynaptic expression of PTP as well as the presynaptic action of the drug.

In summary, we find that Munc13-3 and PKC regulate specific aspects of short-term plasticity at PF synapses. Whereas Munc13-3 regulates initial *p* and thus facilitation, it plays no role in influencing the magnitude or time course of PTP. In contrast, PKC activation appears to be required for PTP, but plays a small role in regulating facilitation and initial *p*. Thus, distinct presynaptic mechanisms appear to control initial *p*, short-term enhancement during trains and post-tetanic potentiation at PF terminals.

Discussion

Our major finding is that for synapses made by cerebellar granule cells, two specific mechanisms of short-term plasticity are regulated in a target-dependent manner. PCs regulate PF synapses by releasing eCBs, whereas GCs do not. PTP, mediated by the

activation of PKC, is also more prominent at PF→PC synapses than at PF→GC synapses. As a result, PF→PC synapses can be continuously regulated from prominent enhancement to strong suppression, whereas PF→GC synapses exhibit little plasticity following stimulus trains.

Target-dependence of endocannabinoid signaling

The observed target-dependence of eCB signaling represents a novel mechanism of attaining synapse specificity. Previous studies established that eCBs can regulate different types of neurons based on the expression pattern of presynaptic CB1Rs (Bodor et al., 2005; Martin et al., 2001; Trettel et al., 2004; Wilson et al., 2001). Here we describe a very different type of synapse specificity where CB1Rs are ubiquitously expressed on PF terminals, but only some types of target neurons are able to release eCBs sufficiently to regulate synaptic strength. The target dependence of SSE at PF synapses is consistent with the prominent role of mGluR1s in SSE. At all PF synapses where eCB-mediated changes in synaptic strength are observed, including PF→PC (Brown et al., 2003) and PF-to-stellate cell synapses (Beierlein and Regehr, 2006; Soler-Llavina and Sabatini, 2006), glutamate released from PFs activates mGluR1, which in turn leads to the activation of PLCβ and DAG lipase, and the production of the endocannabinoid 2-AG (Safo et al., 2006). 2-AG then reduces the probability of neurotransmitter release by activating presynaptic CB1Rs that in turn inhibit presynaptic calcium channels (Brown et al., 2004). In contrast, most GCs do not express mGluR1s (Knoflach et al., 2001; Watanabe and Nakanishi, 2003), consistent with the lack of SSE at PF→GC synapses.

While SSE and DSE are absent at PF→GC synapses, exogenous CB1R agonists inhibit release at these synapses, pointing to the inability of GCs to release eCBs as the underlying reason for the lack of eCB signaling, rather than the lack of presynaptic CB1Rs. The absence of SSE at GC synapses during activation and eCB release at nearby neurons indicates that GC synapses are functionally isolated from eCB signaling in cerebellar circuits.

Target-dependence of PTP

The large difference in the magnitude of PTP at synapses on PCs and GCs is the first example of a target-specific regulation of PTP. Several lines of evidence suggest that this difference is not a consequence of differences in the initial *p*. First, in rats the similarity in the magnitude of facilitation at synapses onto PCs and GCs suggests that *p* is similar at synapses onto these two targets. Second, differences in PTP between GCs and PCs remain prominent even when the initial *p* is reduced by lowering external calcium. Third, differences in PTP remain in the presence of the low affinity glutamate receptor antagonist DGG, indicating that postsynaptic factors such as AMPA receptor saturation do not contribute to differences in PTP. In wild-type mice synapses onto GCs displayed less paired-pulse facilitation compared to synapses onto PCs. However, even though Munc13-3 deletion in mice resulted in significant changes in paired-pulse facilitation and thus initial *p* at both synapses, the magnitude of PTP at both synapses remained the same, suggesting that initial *p* and PTP are regulated independently.

Several mechanisms could explain the target-dependent differences in PTP. First, synapses onto GCs and PCs might display differences in presynaptic calcium signals. However, synapses onto GCs and PCs displayed paired-pulse facilitation with a similar magnitude and time course. As the properties of paired-pulse facilitation are controlled by presynaptic calcium (Atluri and Regehr, 1996; Kamiya and Zucker, 1994; Katz and Miledi, 1968; Zucker, 1996; Zucker and Regehr, 2002) calcium signals evoked by single stimuli are likely to be similar for the two synapses, contrary to what was observed for cortical synapses that displayed target-dependent differences in initial *p* (Koester and Johnston, 2005; Rozov et al.,

2001). It remains possible that the properties of presynaptic calcium signals following bursts show target-dependent differences. Second, PKC signaling might be different at the two PF synapses, either mediated by differences in the concentration or isoforms of PKC, or in the manner in which PKC couples to the release machinery. Further experiments are required to clarify the mechanisms underlying differences in PTP.

Functional consequences of target-dependent short-term plasticity

The ability to independently regulate synaptic strength made by the same presynaptic input enables each type of synapse to interpret the same presynaptic spike train in different ways, thus permitting multiple representations of the same activity pattern. At the PF→PC synapse, bursts of presynaptic activity always result in PTP, regardless of the number and spatial arrangement of activated synapses. Feedback regulation can also occur, but eCB-mediated retrograde signaling is context-dependent in that it relies on the activation of nearby synapses, which permits glutamate pooling and activation of mGluR1s. As a result of the similarity in the time courses of PTP and eCB signaling, retrograde signaling can cancel and eventually overcome the enhancement produced by PTP. This interplay between PTP and eCB release allows the amplitude of burst-induced short-term plasticity to be continuously regulated, with a magnitude that ranges from 20% to 200% of pre-burst amplitudes. Thus, the PF→PC synapse is computationally powerful in that it has a memory of prior activity, with a sign that is context-dependent. PF synapses onto stellate cells share similar properties (Beierlein and Regehr, 2006), indicating that PF-mediated excitation and stellate cell - mediated feed-forward inhibition onto PCs are tightly coordinated. In contrast, the role of the PF→GC synapse appears to be very different, in that regardless of number and spatial arrangement of activated synapses, changes in synaptic strength are more moderate.

The short-term plasticity we observed at PF→GC synapses is consistent with the proposed functional role of GCs in the cerebellar circuitry. GCs integrate a large number of small amplitude excitatory inputs formed by granule cells (Dieudonne, 1998) and in turn form inhibitory contacts with granule cells within glomeruli, a specialized synaptic structure formed by mossy fiber synapses onto granule cell dendrites (Palay and Chan-Palay, 1974). This feedback inhibition mediated by GCs (Eccles et al., 1964; Eccles et al., 1966) is thought to be critical for setting the threshold and controlling the gain of sensory-evoked granule cell activation (Marr, 1969). Thus, the lack of eCB-mediated retrograde signaling and PTP might enable GCs to monitor and in turn regulate the activity of large populations of granule cells in a manner that is insensitive to prior activity.

Experimental procedures

Tissue preparation

Sprague Dawley rats (P14–P18) were anesthetized with halothane, decapitated and transverse cerebellar slices (250 μm) were obtained. Where indicated, transverse slices (200 μm) were obtained from Munc13-3-deficient C57BL6J mice (P13–P15, kindly provided by Kerstin Reim and Nils Brose, Max-Planck-Institute of Experimental Medicine, Göttingen, Germany) or their wild type littermates. All procedures involving animals were approved by the Harvard Medical Area Standing Committee on Animals. Slices were cut in a sucrose-containing solution consisting of (in mM) 81.2 NaCl, 23.4 $NaHCO_3$, 69.9 sucrose, 23.3 glucose, 2.4 KCl, 1.4 NaH_2PO_4, 6.7 $MgCl_2$, and 0.5 $CaCl_2$. Slices were incubated at 32 °C for 30 min and then transferred to a saline solution for 30 min at 32 °C consisting of (in mM) 125 NaCl, 26 $NaHCO_3$, 2.5 KCl, 1.25 NaH_2PO_4, 25 glucose, 2 $CaCl_2$, and 1 $MgCl_2$. Experiments were performed at 33–34 °C using an in-line heater (Warner, Hamden, CT)

while perfusing the bath with saline solution at 3–4 ml/min using a Minipulse 3 pump (Gilson, Middleton, WI).

Electrophysiology

Whole cell recordings of PCs and GCs were obtained using pipettes of 1.2 to 2 MΩ resistance. Cells were visualized using differential interference contrast optics and a 60x water immersion lens. GCs were identified using previously established criteria (Dieudonne, 1995; Dieudonne, 1998) and distinguished from other types of neurons in the granular layer by the presence of monosynaptic EPSCs evoked by molecular layer stimulation (Bureau et al., 2000). Some cells were filled with an internal solution containing Alexa 594 and their morphology was reconstructed using a 2-Photon microscope (Figure 1H). All cells had an apical dendritic tree that reached into the molecular layer, as well as several basal dendrites that remained in the granular layer (Palay and Chan-Palay, 1974).

For voltage-clamp experiments the internal solution contained (in mM) 127 $CsMeSO_3$, 10 CsCl, 10 HEPES, 0.5 EGTA, 2 $MgCl_2$, 0.16 $CaCl_2$, 2 Mg-ATP, 0.4 NaGTP, and 14 Tris-Creatine phosphate, adjusted to 310 mOsm. For experiments in which cells were held in current clamp the internal solution contained (in mM) 130 $KMeSO_3$, 10 NaCl, 2 $MgCl_2$, 0.16 $CaCl_2$, 0.5 EGTA, 10 HEPES, 4 Na_2ATP, 0.4 NaGTP, and 14 Tris-Creatine phosphate, adjusted to 310 mOsm. Recordings were obtained using a Multiclamp 700A (Molecular Devices, Union City, CA). To stimulate PF inputs, glass electrodes (2–3 MΩ) filled with saline were placed within the inner third of the molecular layer, at lateral distances of >100 μm. Where indicated, spatially dispersed PF inputs were activated by placing a stimulus electrode in the granular layer near the PC layer, at lateral distances of >100 μm to avoid the activation of ascending axons that form synapses onto GCs and PCs under study. Current and voltage clamp recordings were carried out in the presence of picrotoxin (20μM) or bicuculline (20 μM), respectively, to block $GABA_A$-mediated synaptic transmission. The $GABA_B$ receptor antagonist CGP55845 (2 μM) was added in experiments employing brief trains of parallel fiber stimuli. For experiments examining DSI GCs were recorded in sagittal slices using a voltage clamp internal solution containing (in mM) 70 $CsMeSO_3$, 70 CsCl, 10 HEPES, 0.5 EGTA, 2 $MgCl_2$, 0.16 $CaCl_2$, 2 Mg-ATP, 0.4 NaGTP, and 14 Tris-Creatine phosphate, adjusted to 310 mOsm, and IPSCs were evoked at a holding potential of −70 mV, in the presence of NBQX and CPP to block AMPARs and NMDARs, respectively.

To characterize the role of PKC in specific forms of short-term plasticity slices were incubated in 10 μM of the PKC inhibitor GF 109203X for 1 hr. At this concentration we did not observe changes in paired-pulse plasticity (Figures 8A and 8B), suggesting that incubation with the drug did not lead to changes in initial release probability. We also performed measurements of the burst-evoked residual calcium signal (Ca_{res}) in PF terminals using fura-2 AM (Regehr, 2000). In control conditions, Ca_{res} decayed with a time constant τ of 2.6 ± 0.2 s (n=5), significantly faster compared to the decay of PTP (τ = 11.3 s, Figure 4E, cf. Brager et al., 2003). Following incubation in GF 109203X for 1 hr Ca_{res} was largely unchanged in time course (2.6 ± 0.2 s, n=5) and relative magnitude (0.75 ± 0.08 in control, n=5 vs. 0.65 ± 0.04 in GF 109203X, n=5), suggesting that the drug does not interfere with Ca_{res}. To directly test for acute effects of the drug we recorded from PCs in control conditions and then bath-applied GF 109203X. At 10 μM the drug remained ineffective over the recording period (~30 min). When used at a higher concentration (20 μM) we were able to observe a reduction of the PTP magnitude (reduced from 1.84 ± 0.05 in control to 1.36 ± 0.06 following application, n=5) within 30 minutes. However, at this concentration we also observed effects on both paired-pulse plasticity (increased from 2.05 ± 0.05 to 2.32 ± 0.14) and on initial EPSC amplitude (reduced by 22 ± 4%). Therefore, we based our analysis on experiments in which slices were incubated in 10 μM GF 109203X for 1 hr.

Calcium imaging

For calcium measurements in GC dendrites the Cs-based internal solution was supplemented with 500 μM Fura-FF. Fluorescence measurements were obtained at 380 nm and 356 nm excitation using a monochromator (Polychrome IV; TILL Photonics, Gräfelfing, Germany). Fluorescence excitation was limited to a small dendritic region in the molecular layer, including a cell-free area near the dendrite used for background correction. The filter set used was 415 nm dichroic (TILL Photonics) and 515LP for emission (Omega Optical, Brattleboro, VT). Images were acquired with 20 ms exposures at 50 Hz using a SensiCam CCD camera (PCO Computer Optics, Kelheim, Germany). Fura-FF fluorescence ratios were converted to calcium concentration as described previously (Brenowitz et al., 2006), using a K_D for calcium of 3.5 μM (35°C). R_{min} of Fura-FF in the Cs-containing internal solution was measured at 35 °C using a cuvette, in the presence of 0 mM calcium and 4 mM EGTA. R_{max} was determined directly in GCs by bath-applying the calcium ionophore ionomycin (20 μM), in ASCF containing 4 mM calcium.

Data acquisition and analysis

Recordings were digitized at 20 kHz with a 16-bit A/D converter (ITC-16, Instrutech Corp., Port Washington, NY). All analysis was performed using custom macros written in Igor Pro (Wavemetrics, Lake Oswego, OR). Averages are given as mean ± s.e.m.

Acknowledgments

We thank Takashi Sato for help with initial experiments, Kerstin Reim and Nils Brose (MPI of Experimental Medicine, Göttingen, Germany) for providing us with Munc13-3 knockout mice, and members of the Regehr laboratory for comments on the manuscript. Supported by NIH Grants R37NS032405 and R01NS044396 (W.G.R.).

References

Abbott LF, Regehr WG. Synaptic computation. Nature. 2004; 431:796–803. [PubMed: 15483601]

Alle H, Jonas P, Geiger JR. PTP and LTP at a hippocampal mossy fiber-interneuron synapse. Proc Natl Acad Sci U S A. 2001; 98:14708–14713. [PubMed: 11734656]

Atluri PP, Regehr WG. Determinants of the time course of facilitation at the granule cell to Purkinje cell synapse. J Neurosci. 1996; 16:5661–5671. [PubMed: 8795622]

Augustin I, Betz A, Herrmann C, Jo T, Brose N. Differential expression of two novel Munc13 proteins in rat brain. Biochem J. 1999a; 337(Pt 3):363–371. [PubMed: 9895278]

Augustin I, Korte S, Rickmann M, Kretzschmar HA, Sudhof TC, Herms JW, Brose N. The cerebellum-specific Munc13 isoform Munc13-3 regulates cerebellar synaptic transmission and motor learning in mice. J Neurosci. 2001; 21:10–17. [PubMed: 11150314]

Augustin I, Rosenmund C, Sudhof TC, Brose N. Munc13-1 is essential for fusion competence of glutamatergic synaptic vesicles. Nature. 1999b; 400:457–461. [PubMed: 10440375]

Batchelor AM, Garthwaite J. Frequency detection and temporally dispersed synaptic signal association through a metabotropic glutamate receptor pathway. Nature. 1997; 385:74–77. [PubMed: 8985249]

Beierlein M, Regehr WG. Local interneurons regulate synaptic strength by retrograde release of endocannabinoids. J Neurosci. 2006; 26:9935–9943. [PubMed: 17005857]

Betz A, Ashery U, Rickmann M, Augustin I, Neher E, Sudhof TC, Rettig J, Brose N. Munc13-1 is a presynaptic phorbol ester receptor that enhances neurotransmitter release. Neuron. 1998; 21:123–136. [PubMed: 9697857]

Bodor AL, Katona I, Nyiri G, Mackie K, Ledent C, Hajos N, Freund TF. Endocannabinoid signaling in rat somatosensory cortex: laminar differences and involvement of specific interneuron types. J Neurosci. 2005; 25:6845–6856. [PubMed: 16033894]

Brager DH, Cai X, Thompson SM. Activity-dependent activation of presynaptic protein kinase C mediates post-tetanic potentiation. Nat Neurosci. 2003; 6:551–552. [PubMed: 12754518]

Brenowitz SD, Best AR, Regehr WG. Sustained elevation of dendritic calcium evokes widespread endocannabinoid release and suppression of synapses onto cerebellar Purkinje cells. J Neurosci. 2006; 26:6841–6850. [PubMed: 16793891]

Brenowitz SD, Regehr WG. Calcium dependence of retrograde inhibition by endocannabinoids at synapses onto Purkinje cells. J Neurosci. 2003; 23:6373–6384. [PubMed: 12867523]

Brenowitz SD, Regehr WG. Associative short-term synaptic plasticity mediated by endocannabinoids. Neuron. 2005; 45:419–431. [PubMed: 15694328]

Brose N, Hofmann K, Hata Y, Sudhof TC. Mammalian homologues of Caenorhabditis elegans unc-13 gene define novel family of C2-domain proteins. J Biol Chem. 1995; 270:25273–25280. [PubMed: 7559667]

Brose N, Rosenmund C. Move over protein kinase C, you've got company: alternative cellular effectors of diacylglycerol and phorbol esters. J Cell Sci. 2002; 115:4399–4411. [PubMed: 12414987]

Brown SP, Brenowitz SD, Regehr WG. Brief presynaptic bursts evoke synapse-specific retrograde inhibition mediated by endogenous cannabinoids. Nat Neurosci. 2003; 6:1048–1057. [PubMed: 14502290]

Brown SP, Safo PK, Regehr WG. Endocannabinoids inhibit transmission at granule cell to Purkinje cell synapses by modulating three types of presynaptic calcium channels. J Neurosci. 2004; 24:5623–5631. [PubMed: 15201335]

Bureau I, Dieudonne S, Coussen F, Mulle C. Kainate receptor-mediated synaptic currents in cerebellar Golgi cells are not shaped by diffusion of glutamate. Proc Natl Acad Sci U S A. 2000; 97:6838–6843. [PubMed: 10841579]

Chadderton P, Margrie TW, Hausser M. Integration of quanta in cerebellar granule cells during sensory processing. Nature. 2004; 428:856–860. [PubMed: 15103377]

Chevaleyre V, Takahashi KA, Castillo PE. Endocannabinoid-Mediated Synaptic Plasticity in the CNS. Annual Review of Neuroscience. 2006; 29

Delaney AJ, Jahr CE. Kainate receptors differentially regulate release at two parallel fiber synapses. Neuron. 2002; 36:475–482. [PubMed: 12408849]

Delaney KR, Tank DW. A quantitative measurement of the dependence of short-term synaptic enhancement on presynaptic residual calcium. J Neurosci. 1994; 14:5885–5902. [PubMed: 7931551]

Delaney KR, Zucker RS, Tank DW. Calcium in motor nerve terminals associated with posttetanic potentiation. J Neurosci. 1989; 9:3558–3567. [PubMed: 2795140]

Destexhe A, Marder E. Plasticity in single neuron and circuit computations. Nature. 2004; 431:789–795. [PubMed: 15483600]

Dieudonne S. Glycinergic synaptic currents in Golgi cells of the rat cerebellum. Proc Natl Acad Sci U S A. 1995; 92:1441–1445. [PubMed: 7877998]

Dieudonne S. Submillisecond kinetics and low efficacy of parallel fibre-Golgi cell synaptic currents in the rat cerebellum. J Physiol. 1998; 510(Pt 3):845–866. [PubMed: 9660898]

Eccles J, Llinas R, Sasaki K. Golgi Cell Inhibition in the Cerebellar Cortex. Nature. 1964; 204:1265–1266. [PubMed: 14254404]

Eccles JC, Llinas R, Sasaki K. The mossy fibre-granule cell relay of the cerebellum and its inhibitory control by Golgi cells. Exp Brain Res. 1966; 1:82–101. [PubMed: 5910945]

Foster KA, Crowley JJ, Regehr WG. The influence of multivesicular release and postsynaptic receptor saturation on transmission at granule cell to Purkinje cell synapses. J Neurosci. 2005; 25:11655–11665. [PubMed: 16354924]

Gao WJ, Goldman-Rakic PS. Selective modulation of excitatory and inhibitory microcircuits by dopamine. Proc Natl Acad Sci U S A. 2003; 100:2836–2841. [PubMed: 12591942]

Jorntell H, Ekerot CF. Properties of somatosensory synaptic integration in cerebellar granule cells in vivo. J Neurosci. 2006; 26:11786–11797. [PubMed: 17093099]

Kamiya H, Zucker RS. Residual Ca2+ and short-term synaptic plasticity. Nature. 1994; 371:603–606. [PubMed: 7935792]

Katz B, Miledi R. The role of calcium in neuromuscular facilitation. J Physiol. 1968; 195:481–492. [PubMed: 4296699]

Khakh BS, Gittermann D, Cockayne DA, Jones A. ATP modulation of excitatory synapses onto interneurons. J Neurosci. 2003; 23:7426–7437. [PubMed: 12917379]

Knoflach F, Woltering T, Adam G, Mutel V, Kemp JA. Pharmacological properties of native metabotropic glutamate receptors in freshly dissociated Golgi cells of the rat cerebellum. Neuropharmacology. 2001; 40:163–169. [PubMed: 11114394]

Koester HJ, Johnston D. Target cell-dependent normalization of transmitter release at neocortical synapses. Science. 2005; 308:863–866. [PubMed: 15774725]

Kreitzer AC, Regehr WG. Retrograde inhibition of presynaptic calcium influx by endogenous cannabinoids at excitatory synapses onto Purkinje cells. Neuron. 2001; 29:717–727. [PubMed: 11301030]

Losonczy A, Zhang L, Shigemoto R, Somogyi P, Nusser Z. Cell type dependence and variability in the short-term plasticity of EPSCs in identified mouse hippocampal interneurones. J Physiol. 2002; 542:193–210. [PubMed: 12096061]

Maejima T, Hashimoto K, Yoshida T, Aiba A, Kano M. Presynaptic inhibition caused by retrograde signal from metabotropic glutamate to cannabinoid receptors. Neuron. 2001; 31:463–475. [PubMed: 11516402]

Magleby KL. Facilitation, augmentation, and potentiation of transmitter release. Prog Brain Res. 1979; 49:175–182. [PubMed: 42112]

Marcaggi P, Attwell D. Endocannabinoid signaling depends on the spatial pattern of synapse activation. Nat Neurosci. 2005; 8:776–781. [PubMed: 15864304]

Markram H, Gupta A, Uziel A, Wang Y, Tsodyks M. Information processing with frequency-dependent synaptic connections. Neurobiol Learn Mem. 1998a; 70:101–112. [PubMed: 9753590]

Markram H, Wang Y, Tsodyks M. Differential signaling via the same axon of neocortical pyramidal neurons. Proc Natl Acad Sci U S A. 1998b; 95:5323–5328. [PubMed: 9560274]

Marr D. A theory of cerebellar cortex. J Physiol. 1969; 202:437–470. [PubMed: 5784296]

Martin LA, Wei DS, Alger BE. Heterogeneous susceptibility of GABA(A) receptor-mediated IPSCs to depolarization-induced suppression of inhibition in rat hippocampus. J Physiol. 2001; 532:685–700. [PubMed: 11313439]

McNaughton BL. Long-term synaptic enhancement and short-term potentiation in rat fascia dentata act through different mechanisms. J Physiol. 1982; 324:249–262. [PubMed: 7097600]

Ohno-Shosaku T, Tsubokawa H, Mizushima I, Yoneda N, Zimmer A, Kano M. Presynaptic cannabinoid sensitivity is a major determinant of depolarization-induced retrograde suppression at hippocampal synapses. J Neurosci. 2002; 22:3864–3872. [PubMed: 12019305]

Palay, SL.; Chan-Palay, V. Cerebellar Cortex. New York: Springer-Verlag; 1974.

Pelkey KA, Lavezzari G, Racca C, Roche KW, McBain CJ. mGluR7 is a metaplastic switch controlling bidirectional plasticity of feedforward inhibition. Neuron. 2005; 46:89–102. [PubMed: 15820696]

Pouille F, Scanziani M. Routing of spike series by dynamic circuits in the hippocampus. Nature. 2004; 429:717–723. [PubMed: 15170216]

Regehr, WG. Monitoring Presynaptic Calcium Dynamics with Membrane-permeant Indicators. In: Yuste, R.; Lanni, F.; Konnerth, A., editors. Imaging Neurons: A Laboratory Manual. New York: Cold Spring Harbor Laboratory Press; 2000. p. 37.31-37.11.

Reyes A, Lujan R, Rozov A, Burnashev N, Somogyi P, Sakmann B. Target-cell-specific facilitation and depression in neocortical circuits. Nat Neurosci. 1998; 1:279–285. [PubMed: 10195160]

Rosenmund C, Sigler A, Augustin I, Reim K, Brose N, Rhee JS. Differential control of vesicle priming and short-term plasticity by Munc13 isoforms. Neuron. 2002; 33:411–424. [PubMed: 11832228]

Rozov A, Burnashev N, Sakmann B, Neher E. Transmitter release modulation by intracellular Ca2+ buffers in facilitating and depressing nerve terminals of pyramidal cells in layer 2/3 of the rat neocortex indicates a target cell-specific difference in presynaptic calcium dynamics. J Physiol. 2001; 531:807–826. [PubMed: 11251060]

Safo PK, Cravatt BF, Regehr WG. Retrograde endocannabinoid signaling in the cerebellar cortex. Cerebellum. 2006; 5:134–145. [PubMed: 16818388]

Scanziani M, Gahwiler BH, Charpak S. Target cell-specific modulation of transmitter release at terminals from a single axon. Proc Natl Acad Sci U S A. 1998; 95:12004–12009. [PubMed: 9751780]

Shigemoto R, Kinoshita A, Wada E, Nomura S, Ohishi H, Takada M, Flor PJ, Neki A, Abe T, Nakanishi S, Mizuno N. Differential presynaptic localization of metabotropic glutamate receptor subtypes in the rat hippocampus. J Neurosci. 1997; 17:7503–7522. [PubMed: 9295396]

Silberberg G, Grillner S, LeBeau FE, Maex R, Markram H. Synaptic pathways in neural microcircuits. Trends Neurosci. 2005; 28:541–551. [PubMed: 16122815]

Soler-Llavina GJ, Sabatini BL. Synapse-specific plasticity and compartmentalized signaling in cerebellar stellate cells. Nat Neurosci. 2006; 9:798–806. [PubMed: 16680164]

Tempia F, Bravin M, Strata P. Postsynaptic currents and short-term synaptic plasticity in Purkinje cells grafted onto an uninjured adult cerebellar cortex. Eur J Neurosci. 1996; 8:2690–2701. [PubMed: 8996819]

Thomson AM. Activity-dependent properties of synaptic transmission at two classes of connections made by rat neocortical pyramidal axons in vitro. J Physiol. 1997; 502(Pt 1):131–147. [PubMed: 9234202]

Thomson AM. Facilitation, augmentation and potentiation at central synapses. Trends Neurosci. 2000; 23:305–312. [PubMed: 10856940]

Toth K, Suares G, Lawrence JJ, Philips-Tansey E, McBain CJ. Differential mechanisms of transmission at three types of mossy fiber synapse. J Neurosci. 2000; 20:8279–8289. [PubMed: 11069934]

Toullec D, Pianetti P, Coste H, Bellevergue P, Grand-Perret T, Ajakane M, Baudet V, Boissin P, Boursier E, Loriolle F, et al. The bisindolylmaleimide GF 109203X is a potent and selective inhibitor of protein kinase C. J Biol Chem. 1991; 266:15771–15781. [PubMed: 1874734]

Trettel J, Fortin DA, Levine ES. Endocannabinoid signalling selectively targets perisomatic inhibitory inputs to pyramidal neurones in juvenile mouse neocortex. J Physiol. 2004; 556:95–107. [PubMed: 14742727]

von Gersdorff H, Borst JG. Short-term plasticity at the calyx of held. Nat Rev Neurosci. 2002; 3:53–64. [PubMed: 11823805]

Wadiche JI, Jahr CE. Multivesicular release at climbing fiber-Purkinje cell synapses. Neuron. 2001; 32:301–313. [PubMed: 11683999]

Wang J, Zucker RS. Photolysis-induced suppression of inhibition in rat hippocampal CA1 pyramidal neurons. J Physiol. 2001; 533:757–763. [PubMed: 11410632]

Watanabe D, Nakanishi S. mGluR2 postsynaptically senses granule cell inputs at Golgi cell synapses. Neuron. 2003; 39:821–829. [PubMed: 12948448]

Wierda KD, Toonen RF, de Wit H, Brussaard AB, Verhage M. Interdependence of PKC-Dependent and PKC-Independent Pathways for Presynaptic Plasticity. Neuron. 2007; 54:275–290. [PubMed: 17442248]

Wilson RI, Kunos G, Nicoll RA. Presynaptic specificity of endocannabinoid signaling in the hippocampus. Neuron. 2001; 31:453–462. [PubMed: 11516401]

Zucker RS. Exocytosis: a molecular and physiological perspective. Neuron. 1996; 17:1049–1055. [PubMed: 8982154]

Zucker RS, Regehr WG. Short-term synaptic plasticity. Annu Rev Physiol. 2002; 64:355–405. [PubMed: 11826273]

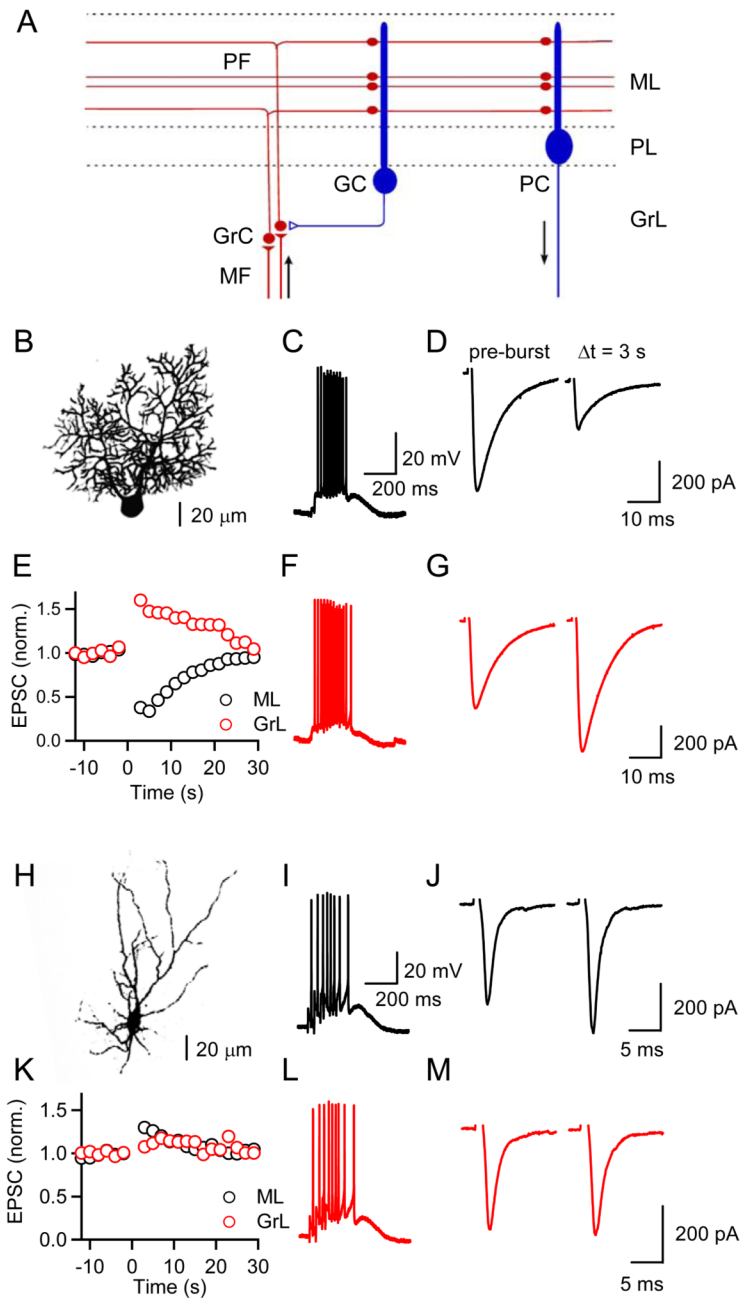

Figure 1. Target cell-specific short-term enhancement and suppression at parallel fiber synapses

(A) A simplified circuit of the cerebellar cortex shows excitatory synapses made by granule cell (GrC) parallel fibers (PFs) onto Purkinje cells (PCs) and Golgi cells (GCs). Arrows indicate that mossy fibers (MFs) provide a major source of excitatory input to the cerebellar cortex and PCs are the sole output from this region. ML, molecular layer; PL, Purkinje cell layer; GrL, granular layer. (B, H) Fluorescent images of a PC (B) and a GC (H) filled with Alexa 594. Postsynaptic responses to PF burst stimulation (10 stimuli, 50 Hz) were recorded in current clamp (C, F, I, L). PFs were activated with an extracellular electrode placed either in the ML (C, D, I, J, *black traces*) or the GrL, (F, G, L, M, *red traces*). EPSCs evoked at 0.5 Hz prior to and following a PF burst were recorded in voltage-clamp, at a holding

potential of −70 mV in a representative PC (D, G) and a GC (J, M), using a K-based internal solution. (E, K) Time course of change in synaptic strength following PF bursts (at t = 0 s) evoked by ML (*black*) or GrL stimulation (*red*). Responses shown are normalized to the average EPSC amplitude prior to burst stimulation.

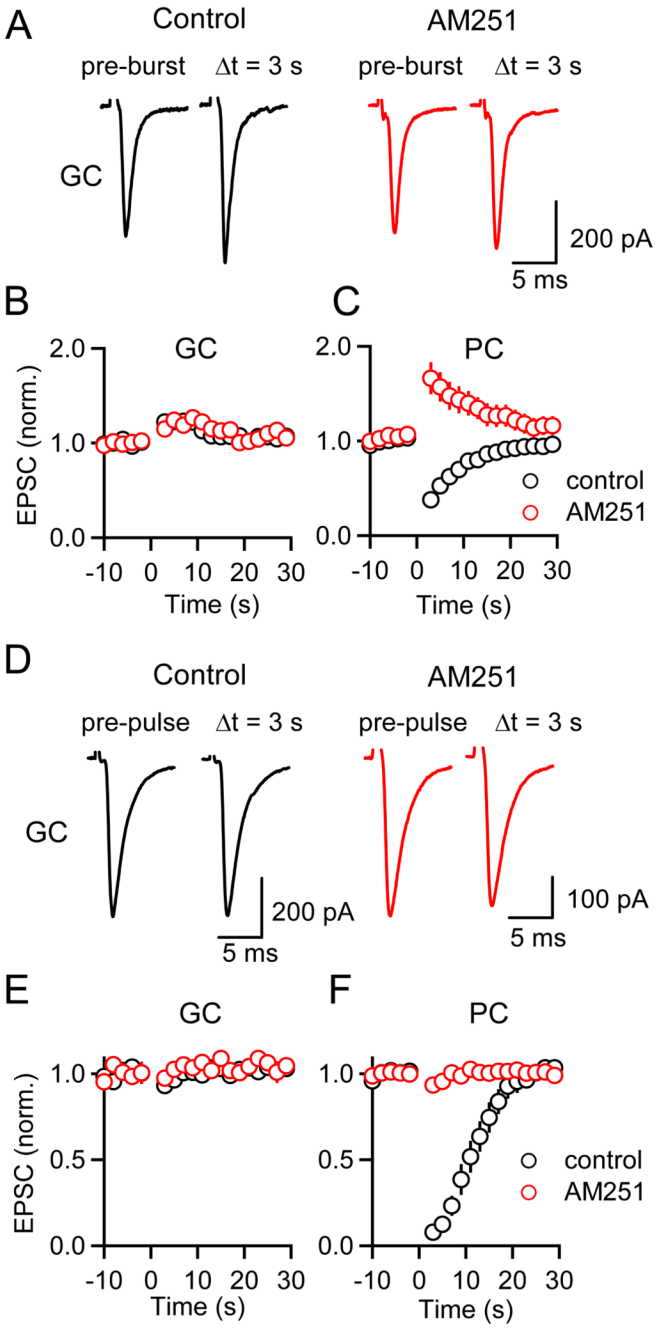

Figure 2. Target cell-dependent short-term suppression is mediated by endocannabinoids

Synaptically-evoked suppression of excitation (SSE; A, B) and depolarization-induced suppression of excitation (DSE; D, E) were examined at PF→GC synapses. Summary data of PC SSE (C) and DSE (F) are shown for comparison. Experiments were performed in control conditions (*black traces and black symbols*) and in the presence of the CB1R antagonist AM251 (2 μM, *red traces and red symbols*). Studies of SSE were performed using a K-based internal solution and PFs were stimulated in the ML. Studies examining DSE were performed with a Cs-based internal solution. (A) EPSCs recorded from a GC, evoked prior to (pre-burst) and 3 s following PF burst stimulation. Time course of EPSC amplitudes prior to and following burst stimulation is shown for synapses onto GCs (B; n =

5 cells in control, n = 5 cells in AM251) and PCs (C; n = 6 cells in control, n = 5 cells in AM251). (D–F) Cells were depolarized to 0 mV for 2 s. Representative recordings are shown for a GC (D) and the time course of synaptic strength prior to and following postsynaptic depolarization is shown for GCs (E; n = 15 cells in control, n = 7 cells in AM251) and PCs (F; n = 7 cells in control, n = 6 cells in AM251). Figures 2C and 2F reproduced from (Beierlein and Regehr, 2006) to allow comparison.

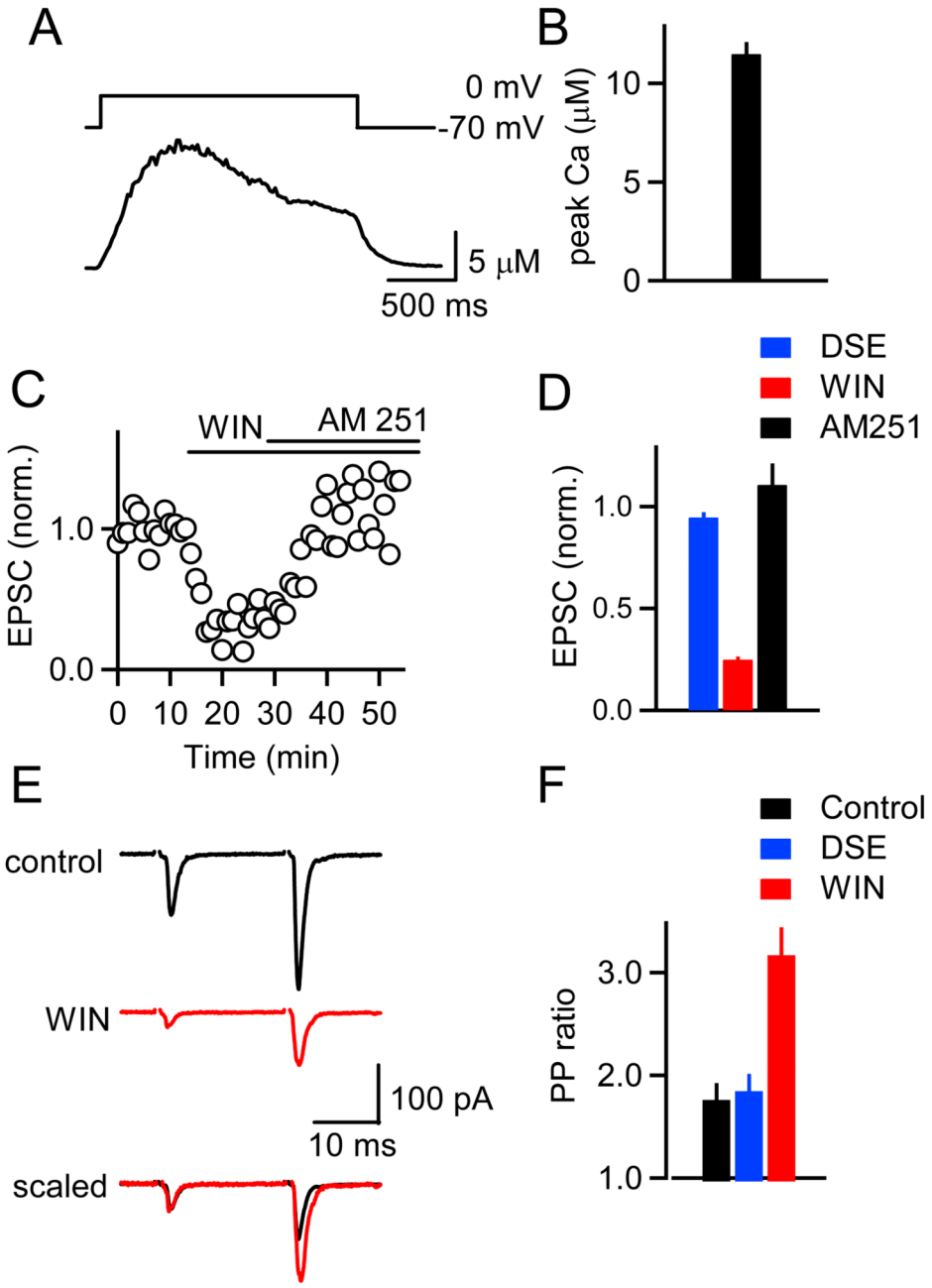

Figure 3. Calcium signals in GC dendrites and presynaptic expression of CB1R at PF to GC synapses

(A) A representative experiment is shown in which a GC was voltage-clamped, depolarized from −70 mV to 0 mV for 2 s, and the resulting dendritic calcium signal was quantified with Fura-FF. (B) Average peak dendritic calcium levels measured in 6 GCs. (C) Bath application of the CB1R agonist WIN 55,212-2 (WIN, 2 μM) reduces the amplitude of PF→GC EPSCs. EPSC amplitude is restored following bath application of AM251 (5 μM). (D) Summary of the effects of a 2 s depolarizing step (DSE, *blue*), WIN (*red*) and of AM251 (*black*) on the magnitude of the EPSC in GCs (n = 5). (E–F) Effects of postsynaptic depolarization and WIN on paired-pulse facilitation (20 ms ISI). Experiments were

conducted in 4 mM external calcium. As shown for a representative experiment (E), WIN reduced the amplitude of the first and second EPSC. Overlay, with the traces scaled to the amplitude of the first response, shows that WIN increased pairedpulse facilitation. (F) Summary of the average paired-pulse ratio (PPR = $EPSC_2/EPSC_1$) in control conditions (*black*), following a 2 s depolarization (*blue*), and following WIN application (*red*, n = 5 GCs).

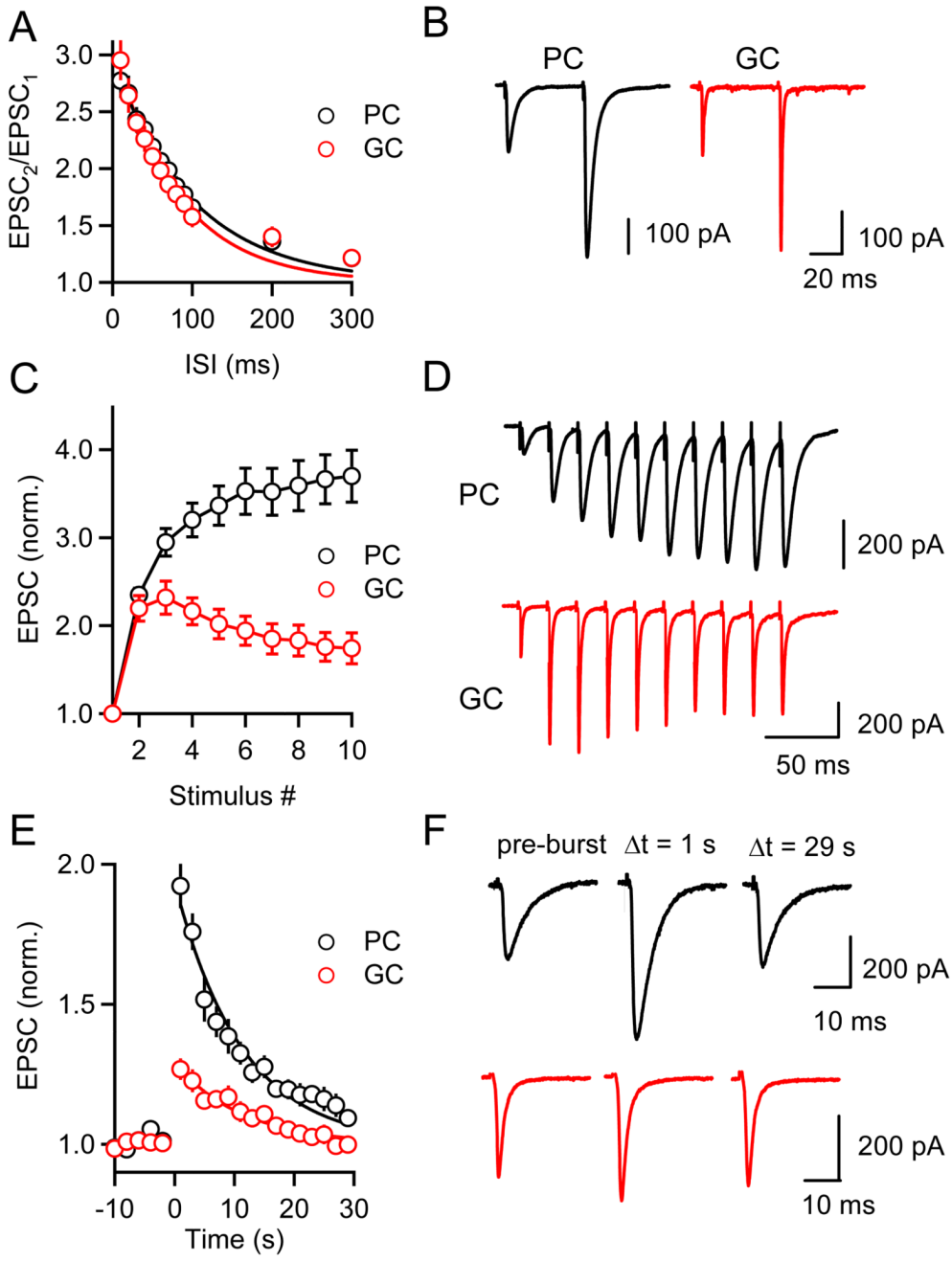

Figure 4. Target-dependent differences in short-term facilitation and PTP

Paired-pulse facilitation (A, B), enhancement during stimulus trains (C, D), and PTP (E, F) following stimulus trains (10 stimuli at 50 Hz) were examined at PF synapses onto PCs (*black*) and GCs (*red*). EPSCs were recorded in voltage-clamp with a Cs-based internal solution in the presence of $GABA_AR$, $GABA_BR$, and CB1R antagonists. Summaries of experiments examining each form of plasticity (A, n = 6 PCs and GCs; C, n = 13 PCs and GCs; E, n = 12 PCs and GCs) and representative experiments (B, D, F) are shown.

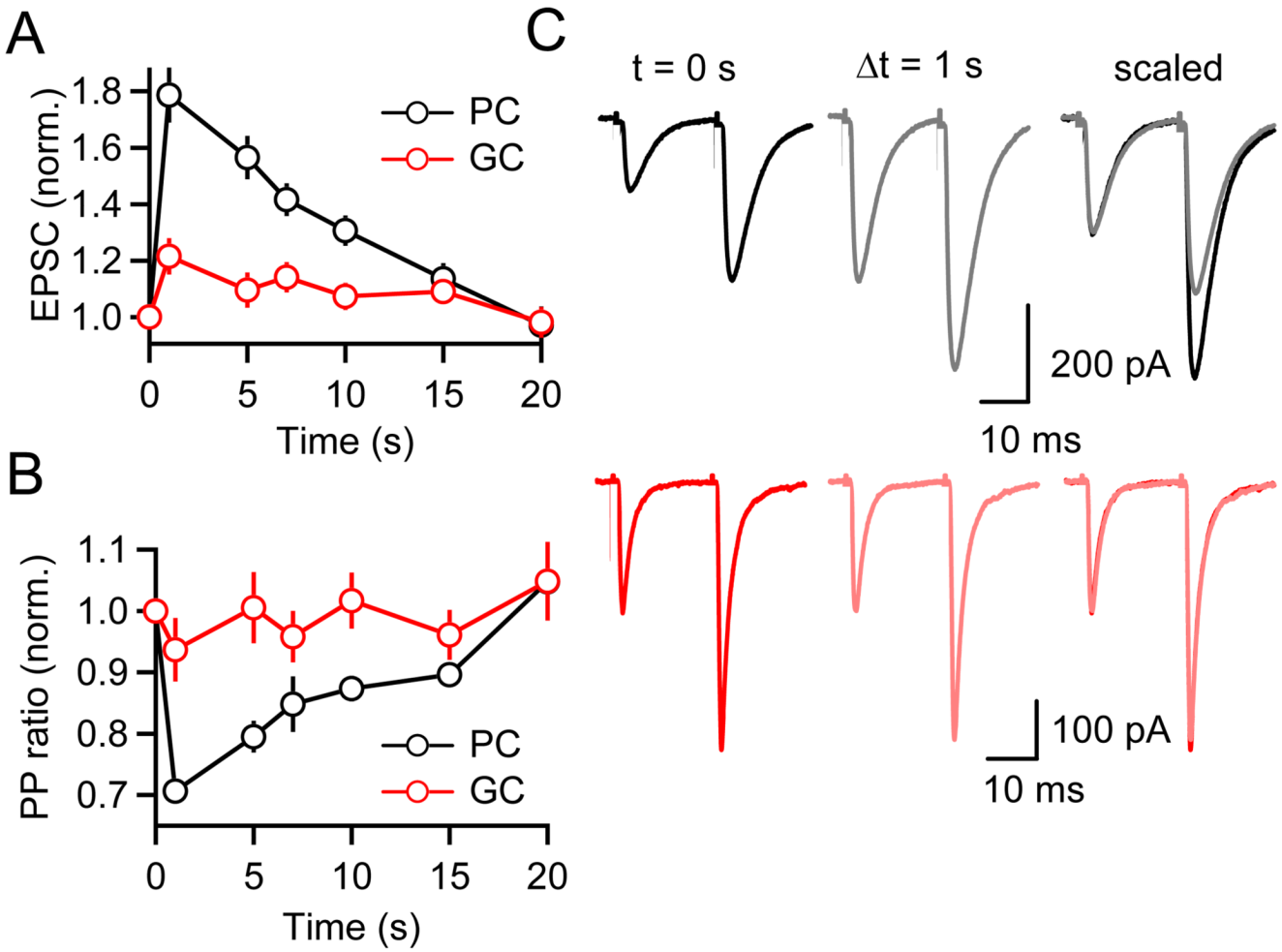

Figure 5. PTP at PF synapses is expressed presynaptically

The magnitude of PTP (A, C) and changes in paired-pulse ratio ($EPSC_2/EPSC_1$) during PTP (B, C) were determined following PF bursts (10 stimuli at 50 Hz). (A) Summary of magnitude of PTP, with responses normalized to $EPSC_1$ of the burst (n = 9 PCs, n = 14 GCs). (B) Changes in PPR, for the same data set shown in (A).Values are normalized to PPR at time t = 0 s. Representative experiments (C) are shown for synapses onto PCs (*black*) and GCs (*red*).

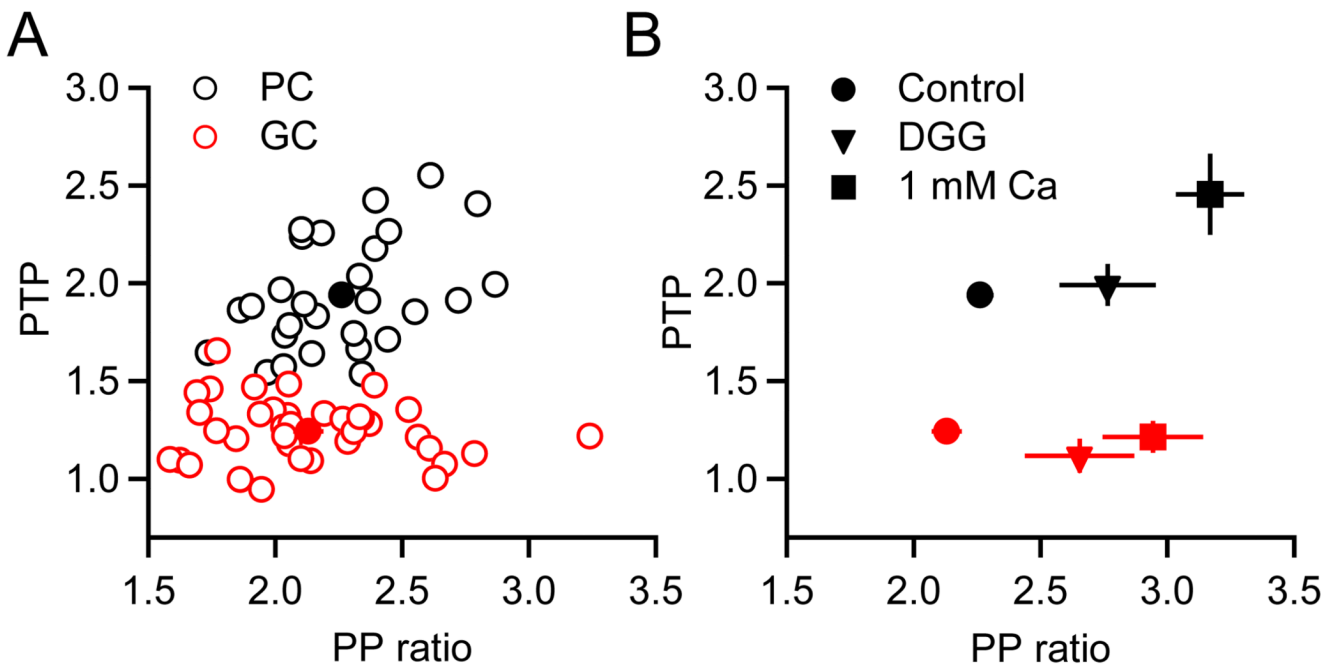

Figure 6. Target-specific differences in PTP do not depend on initial release probability

(A) Graph plots the magnitude of PTP (EPSC amplitude at Δt = 1 s following burst, normalized to EPSC prior to burst) as a function of paired-pulse ratio for PCs (n = 28, *black symbols*) and GCs (n = 38, *red symbols*). Filled symbols denote average values. (B) Average values for PTP and paired-pulse ratio for control conditions (*circles*, same as (A)), 2 mM DGG (*triangles*, n = 6 PCs, n = 8 GCs) and 1 mM external calcium (*squares*, n = 6 PCs, n = 6 GCs), for PCs (*black*) and GCs (*red*).

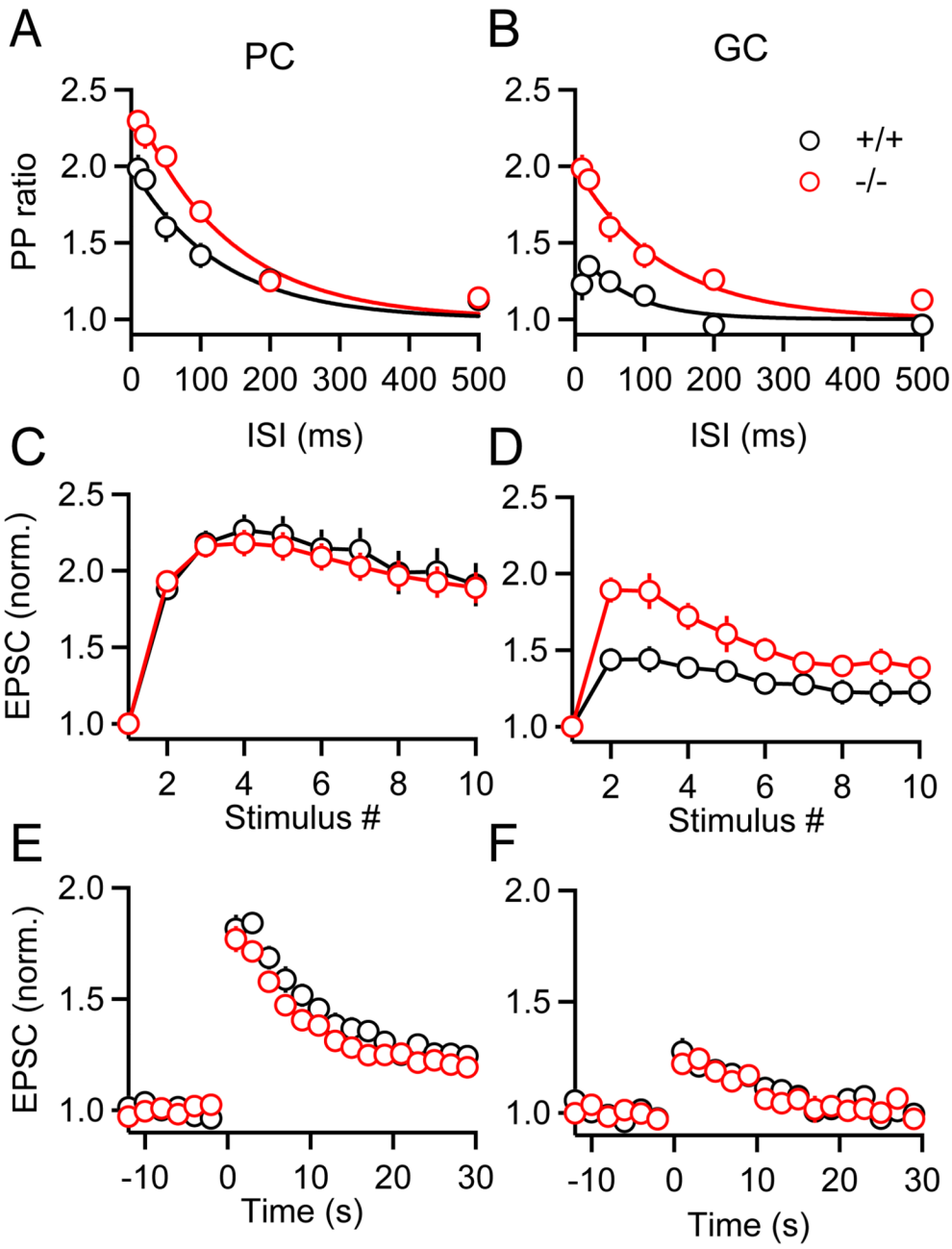

Figure 7. Munc13-3 modulates paired-pulse plasticity without influencing PTP

Short-term plasticity was examined in Munc13-3 knockout mice (*red traces*) and their wild-type littermates (*black traces*). Summaries are shown for PPR ($EPSC_2/EPSC_1$) measured for a range of inter-stimulus intervals for PCs (A) and GCs (B) (n = 4 to 6 for each condition). Summary data for enhancement during (C, D) and following (E, F) PF bursts (10 stimuli, 50 Hz) (n = 10 to 16 cells for each condition).

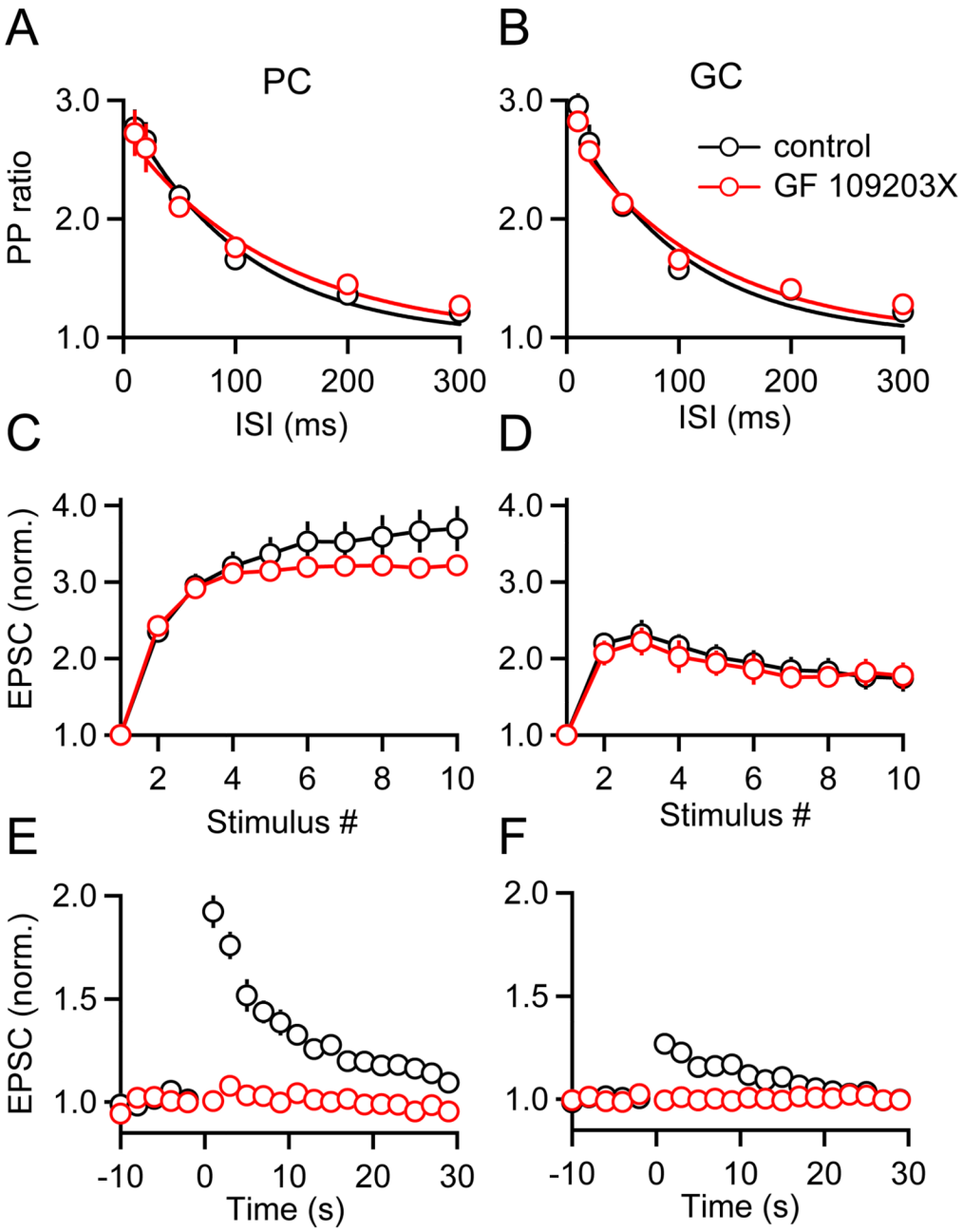

Figure 8. PKC is required for PTP

Paired-pulse plasticity (A, B), enhancement during (C, D), and following (E, F) stimulus trains (10 stimuli, 50 Hz) were examined at PF synapses onto PCs and GCs, in control conditions (*black symbols*) and in the presence of the protein kinase C (PKC) inhibitor GF 109203X (10 μM, *red symbols*, n = 7 PCs, n = 6 GCs). 3 0